Evolution of infrared modes across the insulator to metal transition in manganites

M. Premila[1], T. N. Sairam[1] and C. S. Sundar[1,2]*

[1]Materials Science Division, Indira Gandhi Centre for Atomic Research, Kalpakkam 603 102, India
[2]Jawaharlal Nehru Centre for Advanced Scientific Research, Bangalore 560 064, India

Low temperature infrared absorption measurements have been carried out on polycrystalline samples of $La_{.67}Ca_{.33}MnO_3$ across its insulator-to-metal transition. Significant changes in the mid infrared background and the phonon modes are seen as the system transits to the low temperature metallic phase. The stretching mode is seen to harden and increase in width, as also to develop a Fano asymmetry in the metallic phase. These results are understood in terms of the interaction of the phonons with the changing polaronic background, associated with the insulator to metal transition.

MORE than half a century ago, Jonker and van Santen[1] discovered a striking correlation between magnetic order and conductivity in $La_{1-x}A_xMnO_3$ system, where A is a divalent alkaline earth atom of Ca, Sr or Ba. These manganite alloys are insulating and antiferromagnetic (AFM) at the end points $x = 0$ and $x = 1$ respectively, but in the $0.2 < x < 0.5$ region they are ferromagnetic and metallic. Their crystal structures correspond to those of cubic perovskites or their close variants, with the MnO_6 octahaedron being the important structural motif. The coexistence of metallicity and ferromagnetism in these mixed valent manganites, was rationalized by Zener[2] as arising due to the double exchange (DEX) interaction, wherein the simultaneous hopping of e_g electrons between the Mn^{3+} and Mn^{4+} ions, through the intervening oxygen atom, is favoured for the ferromagnetic alignment of core spins due to t_{2g} electrons, because of strong Hund's rule coupling. Another interesting aspect of the manganites accrues from the fact that Mn^{3+} is a Jahn–Teller ion, and the consequent elastic distortions of the $Mn^{3+}O_6$ octahedron play an important role in influencing the evolution of magnetic and structural phase diagram, as was appreciated early on[3].

The recent resurgence of interest in these manganites, follows the discovery[4] of colossal magnetoresistance, viz. a huge magnetic field induced reduction in the resistivity. These materials also exhibit a variety of interesting properties that are related to the interplay of the spin, charge and lattice degrees of freedom[5]. The insulator to metal transition in these manganites, that is correlated with the paramagnetic to ferromagnetic transition, is governed by the balance between two competing effects: the DEX interaction that increases the electron kinetic energy and hence the delocalization, and the strong Jahn–Teller coupling that tends to localize the carrier in a local lattice distortion, viz. the formation of lattice polarons[6,7]. Evidence for the formation of polarons in manganites has been obtained by probing local structural distortions of the MnO_6 octahedron using diffraction, EXAFS and pair distribution measurements[8–10]. Optical studies, including both infrared[11–14] and Raman spectroscopy[15,16], have proved very valuable in the study of manganites. These studies have pointed to the important role played by the MnO_6 vibrations, and that the insulator to metal transition is associated with a crossover from Jahn–Teller small polarons in the paramagnetic state to their coherent motion in the ferromagnetic phase[14].

Since the infrared phonon spectra are sensitive to these local distortions[11], it is of interest to follow the phonon modes across the metal–insulator transition. Here we report on the low temperature infrared absorption measurements on polycrystalline samples of $La_{.67}Ca_{.33}MnO_3$ (LCMO) across the metal–insulator transition. In the present study, we follow the correlated variation of the mid infrared band, that is associated with the polaronic absorption, and the internal modes of MnO_6 octahedron, in particular the high frequency stretch mode. Our principal observations are that this stretch mode exhibits a significant hardening and broadening below the insulator to metal transition. We also observe that this stretch mode develops an asymmetric Fano lineshape[17] below the transition. These results are compared with the results of earlier studies[11,13] and discussed in the light of theoretical calculations by Lee and Min[18], who have explored the influence of DEX interaction on lattice vibrations. In addition to the studies on stretch mode, we have also followed the temperature dependence of the Mn–O bending mode and the long wavelength lattice mode located at ~190 cm^{-1}, that corresponds to the vibration of La/Ca ions against the MnO_6 octahedra[11].

Experimental details

Polycrystalline powder samples of $La_{.67}Ca_{.33}MnO_3$ have been prepared by mixing stoichiometric proportions of La_2O_3, $CaCO_3$ and MnO_2; subjecting them to programmed heat treatment in air in the temperature range of 1000–1400°C for 72 h, followed by grinding, and a final heat

*For correspondence. (e-mail: css@igcar.ernet.in)

treatment at 1500°C in an oxygen atmosphere for 36 h. Resitivity and susceptibility measurements indicate a paramagnetic insulator to ferromagnetic metal transition below 255 K. Infrared absorption measurements were carried out on well characterized, finely ground samples using a Bomem-DA8 FTIR spectrophotometer operating with a resolution of 4 cm^{-1}. Measurements in the far infrared (FIR) range were carried out using an extended 6 micron mylar beam splitter and deuterated triglycine sulfate (DTGS) detector in the range 30–900 cm^{-1} on samples pelletized with high density polyethylene powder. In addition, we have carried out measurements in the mid infrared (MIR) range of 400–4000 cm^{-1} using a combination of KBr beam splitter and a mercury cadmium telluride (MCT) detector on samples pelletized with KBr. For experiments involving temperature variation of the infrared modes, the pellets were mounted inside a JANIS continous flow cryostat and studies in the temperature range of 80 K–300 K were carried out.

Results and discussions

Room temperature infrared absorption spectra of the sample revealed the expected[11] three infrared active modes at 590 cm^{-1}, 390 cm^{-1} corresponding to the stretching and the bending modes of the MnO_6 octahedra respectively, and a lattice mode at ~190 cm^{-1}, that represents the motion of the MnO_6 unit with respect to the metal ion. Figure 1 shows the infrared absorption in the MIR range indicating the sharp absorption feature at ~ 590 cm^{-1} due to the stretch mode vibrations superposed on the broad background due to the polaronic absorption[11,13]. With lowering of temperature, in particular, below the insulator to metal transition temperature of 255 K, the absorption background is seen to increase. Associated with this, the oscillator strength of absorption mode at 590 cm^{-1} is seen to decrease. This decrease in the intensity of the stretch mode and build up in the intensity of the broad MIR band, which are correlated with the insulator to metal transition at 255 K are shown in the insets (*a*) and (*b*) of Figure 1. With lowering of temperature, a hardening of the stretch mode and an increase in its width can also be discerned. Further, the stretch mode is seen to become more asymmetric below the insulator to metal transition. This is shown in more detail in the inset (*c*) of the figure. Such an asymmetry towards higher wave numbers reflects the interaction of the discrete phonon mode with a continuum of states on the high energy side, and hence we have fitted this absorption feature to the Fano lineshape[17].

$$I = I_0\{1 + [(\omega - \omega_0)/\Gamma q]\}^2/\{1 + (\omega - \omega_0)^2/\Gamma^2\},$$

where ω and ω_0 are the renormalized and bare phonon frequencies respectively. $1/q$, the asymmetry parameter, is a measure of the strength of the coupling between the discrete mode and a continuum, and Γ is the width of the resonance interference between the continuum and the discrete channels. The resulting parameters of this analysis are shown in Figure 2. It is seen that below the insulator to metal transition, there is a sharp increase in the phonon frequency (ω) and line width (Γ). Further the asymmetry parameter '$1/q$' is also seen to dramatically increase as the system transits to the metallic phase.

The results shown in Figure 1 are similar to those of the earlier absorption studies on LCMO ($x = 0.25$) by Congeduti *et al.*[13] who have also observed an increase in the intensity of the MIR band associated with the polaronic absorption, and an associated reduction in the absorption feature due to stretch mode that is due to the screening by charge carriers. The effective number of carriers, obtained by them by integrating the region beyond 750 cm^{-1} bears a strong resemblance to the inset (b) in Figure 1. However, in these studies[13], the variation of phonon frequency with temperature has not been followed in detail, as has been done in the present investigations. The hardening of the stretch mode, as seen in the top panel of Figure 2*a* is similar to the results of Kim *et al*[11], which provided the early evidence for the involvement of polarons in the insulator to metal transition in manganites. However, in their studies[11], the corresponding variation in linewidths was not indicated. The present study goes beyond these earlier investigations, by monitoring changes in all the phonon lineshape parameters, along with that of the background. Further, the need for fitting to the Fano lineshape, and its implications have not been explored in the earlier studies.

On the theoretical front, Lee and Min[18] have explored the effect of DEX interaction on the vibrational degrees of freedom. According to their model, the DEX factor $\gamma = \langle\cos\theta/2\rangle$, that modifies the hopping matrix element of carriers between neighbouring sites depending on the angle θ between the spins, alters the screening of the phonons leading to a hardening of the phonon modes below T_c. These detailed calculations also indicate that correspondingly the phonon linewidth should decrease as $1/\gamma^2(T)$, as $\gamma(T)$ increases in the ferromagnetic metallic phase. This, however, is not borne out by experimental results as shown in Figure 2*b*. In fact, the linewidth has an opposite behaviour, viz. an increase in the metallic phase.

In the following, we try to explore the plausible reasons for observed changes in the lineshape parameters. Apriori, the hardening of the stretch mode as seen in Figure 2*a*, could be a reflection of the reduction in the Mn–O bond lengths that occurs[8] across the insulator to metal transition. From the experimentally determined[8] values of Mn–O bond lengths and lattice volume, V, and the value[16] of the Gruneisen parameter, viz. $\delta\ln(\omega)/\delta\ln(V) = 2$, for the high frequency Raman mode, we have estimated the expected hardening of the stretch mode frequency. These are indicated by the dotted line in Figure 2*a*. The observed large increase in the phonon frequency cannot be rationalized in terms of the reduction in Mn–O bond length or unit cell

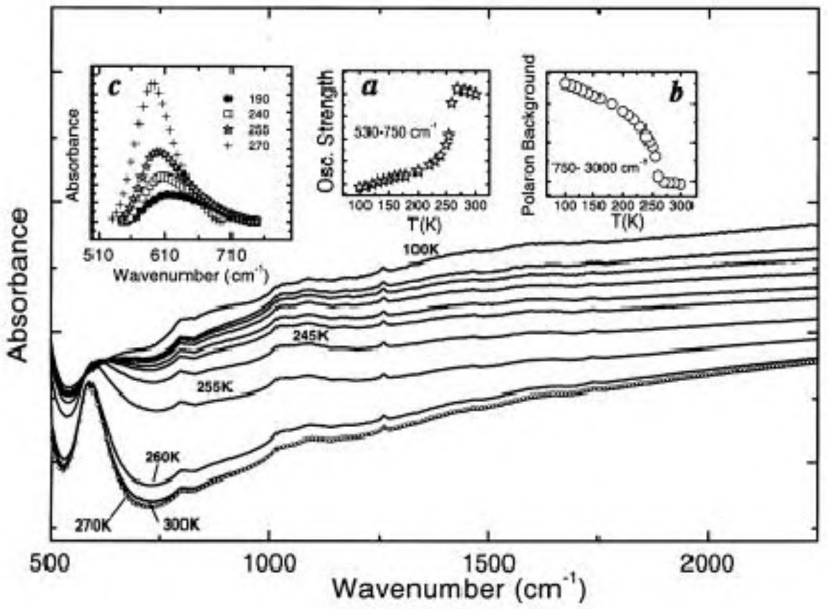

Figure 1. Low temperature MIR absorption in $La_{.67}Ca_{.33}MnO_3$. The increase in the background absorption and the decrease in oscillator strength of stretch mode with lowering of temperature, is clearly seen. The correlated decrease in phonon oscillator strength (530–750 cm^{-1}) and the associated increase in polaronic background (750–3000 cm^{-1}) across the insulator–metal transition are shown in insets (*a*) and (*b*) respectively. Also shown in inset (*c*) is the evolution of the asymmetric Fano lineshape of the stretch mode.

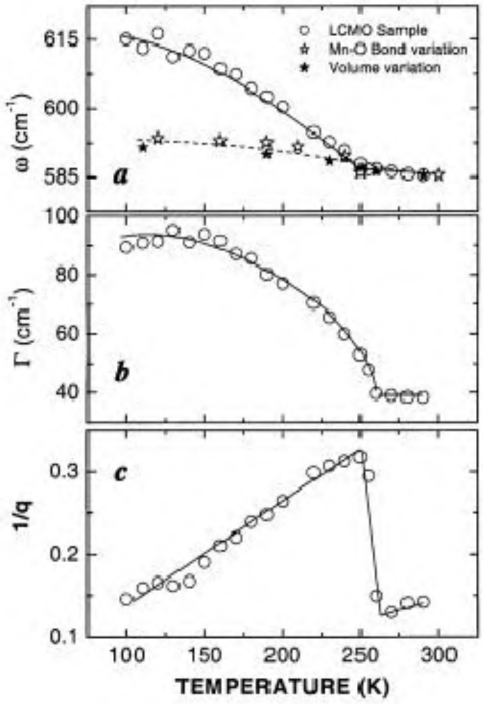

Figure 2. Temperature variation of the stretch mode lineshape parameters in LCMO. Panel (*a*) shows the hardening of the phonon mode below the insulator to metal transition. The expected variation based on the observed changes in Mn–O bond lengths and lattice volume (see text) are indicated by the dotted line. Panels (*b*) and (*c*) show the variation in phonon linewidth, Γ, and the asymmetry factor, 1/*q* across the insulator to metal transition at ~255 K. The continuous lines are drawn as guides to the eye.

volume. The large variation in the mode frequency that is associated with changes in linewidth and the Fano lineshape points to an electronic origin for this effect. It is well known that in conventional metallic systems, the self energy of the phonon interacting with free carriers results in softening and broadening of the phonon mode[19]. In the present case, however, we observe a hardening of the stretch mode that is associated with an increase in linewidth (cf. Figure 2). This may be attributed to the interaction of the phonon mode with an electronic continuum on the high energy side, viz. the polaronic band. Such an interaction of the stretch mode with the MIR polaronic band, as compared with the Drude peak, can also account for development of Fano asymmetry on the high frequency side. The subsequent reduction of the Fano interaction parameter, 1/*q*, in the metallic phase (cf. Figure 2 *c*) may be related to the down-shifting of the polaron band with the lowering of temperature[12,14]. Thus, by invoking the phonon–polaron interaction, we can qualitatively account for all the observed features in Figure 2. We must mention here that we have also observed similar temperature dependence of phonon parameters in a related system, namely, Ti-doped $La_{67}Ca_{33}Mn_{.99}Ti_{.01}O_3$ having a lower transition temperature of 240 K (figures not shown) and these provide additional support for results shown in Figure 2. These point to the need to go beyond the phonon–DEX interaction[18] to understand the behaviour of phonons in manganites. Evidence for interaction of phonons with the changing polaronic background has also been observed[20] in the high temperature superconductor, $Nd_{1.96}Ce_{0.04}CuO_{4+y}$.

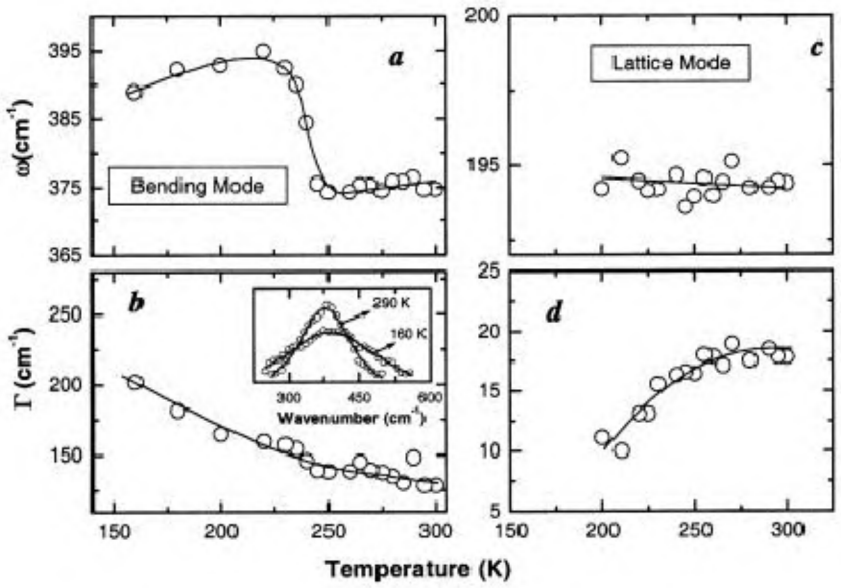

Figure 3. Variation of mode parameters with temperature for the bending and lattice modes in LCMO, as obtained by a single component Lorentzian fit. (*a*) Bending mode frequency, (*b*) Width of the bending mode. The inset shows the bending mode at 290 K and 160 K, along with the Lorentzian fits. Panels (*c*) and (*d*) show the temperature dependence of the frequency and linewidth of the lattice mode.

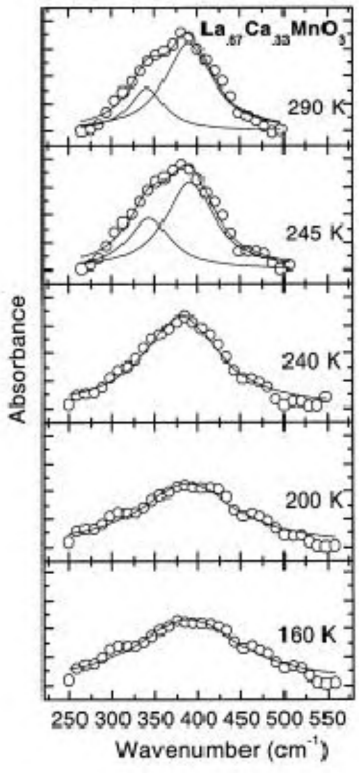

Figure 4. Variation of bending mode with temperature. Note that the two component spectrum in the high temperature insulating phase evolves to a single broad component in the low temperature metallic phase.

The infrared absorption due to bending mode vibrations in manganite is characterized by a broad feature centred at 375 cm^{-1}, with a width ~ 125 cm^{-1} (see inset in Figure 3). With the lowering of temperature, this is seen to broaden further and shift towards higher wave number. It is seen that this mode does not exhibit any discernable asymmetry, unlike the stretch mode (cf. Figure 1 *c*). This lack of Fano asymmetry together with a large linewidth, as compared to the stretch mode, may arise due to the interaction of the bending mode with both the Drude peak that picks up below 350 cm^{-1} on the low energy side[12,14] and the MIR polaronic band. We have analysed the bending mode in terms of a single Lorentzian, and the resulting temperature dependence of the mode frequency and width are shown in Figure 3*a* and *b* respectively. A sharp increase in the mode frequency, associated with the insulator to metal transition is seen, similar to the earlier observations by Kim *et al.*[11]. In addition, we observe an increase in linewidth in the metallic phase, as was also seen in the case of the stretch mode (cf. Figure 2), and this is counter to the theoretical predictions of Lee and Min[18].

We note that the large linewidth of the bending mode could also be a reflection of microscopic inhomogeneities[21] in the distribution of Mn^{3+} and Mn^{4+} ions, since the bending mode vibrations can be expected to be more sensitive to local structural variations. With this premise, we have fitted the bending mode absorption feature to two components as shown in Figure 4. It is seen that the two components seen for the insulating phase collapse into a single broad

component below T_c. Physically, this can be attributed to the presence of two discrete Mn^{3+} and Mn^{4+} environments in the insulating phase that get smeared in the low temperature metallic region due to the mobility of holes. In order to have a definitive understanding of the origin of large linewidth of the bending mode, as to whether it arises due to microscopic inhomogeneities or is an indication of the interaction of the bending mode with the continuum of electronic excitations, further studies on other doped manganites would be instructive.

In contrast to these interesting temperature dependence of the internal modes of the MnO_6 octahedra, the lattice mode at $\sim 190\ cm^{-1}$ is seen to exhibit a regular anharmonic trend, as shown in Figure 3 *c* and *d* respectively. These in turn point to the important role played by the local vibrations of MnO_6 octahedra in the metal–insulator transition in manganites[11]. In particular, the present study shows that the stretch mode vibration hardens, increases in width and develops a Fano asymmetry in the metallic phase, and these can be rationalized in terms of the interaction of this IR active mode with the polaronic background.

1. Jonker, G. H. and van Santen, J. H., *Physica* (*Amsterdam*), 1950, **16**, 337.
2. Zener, C., *Phys. Rev.*, 1951, **82**, 403–405.
3. Goodenough, J. B., *Phys. Rev.*, 1955, **100**, 564–573.
4. Jin, S. *et al.*, *Science*, 1994, **264**, 413–415.
5. Salamon, M. B. and Jaime, M., *Rev. Mod. Phys.*, 2001, **73**, 583–628.
6. Millis, A. J., *Nature*, 1998, **392**, 147–150.
7. Roder, H. and Bishop, A. R., *Phys. Rev. Lett.*, 1996, **76**, 1356–1359.
8. Radaeilli, P. G. *et al.*, *Phys. Rev. B*, 1997, **56**, 8265–8276; Radaelli, P. G. *et al.*, *Phys. Rev. Lett.*, 1995, **75**, 4488–4491.
9. Booth, C. H. *et al.*, *Phys. Rev. Lett.*, 1998, **80**, 853–856.
10. Billinge, S. J. L. *et al.*, *Phys. Rev. Lett.*, 1996, **77**, 715–718.
11. Kim, K. H. *et al.*, *Phys. Rev. Lett.*, 1996, **77**, 1877–1880.
12. Kim, K. H. *et al.*, *Phys. Rev. Lett.*, 1998, **81**, 1517–1520.
13. Congeduti, A. *et al.*, *Phys. Rev. B*, 2001, **63**, 184410-1-184410-5.
14. Quijada, M. *et al.*, *Phys. Rev. B*, 1998, **24**, 16093–16102.
15. Yoon, S. *et al.*, *Phys. Rev. B*, 1998, **58**, 2795–2801.
16. Congeduti, A. *et al.*, *Phys. Rev. Lett.*, 2001, **86**, 1251 –1254.
17. Fano, U., *Phys. Rev.*, 1961, **124**, 1866–1878; Zhou, P., *et al.*, *Phys. Rev. B*, 1993, **48**, 8412–8417.
18. Lee, J. D. and Min, B. I., *Phys. Rev. B*, 1997, **55**, 12454 –12459.
19. Allen, P. B., *Solid State Commun.*, 1974, **14**, 937–940.
20. Lupi, S. *et al.*, *Phys. Rev. B*, 1998, **57**, 1248–1252.
21. Dogotto, E., Hotta, T. and Moreo, A., *Phys. Rep.*, 2001, **344**, 1–153.

ACKNOWLEDGEMENTS. We thank Dr V. Sridharan, Ms L. Seethalakshmi and Shri D. V. Natarajan for the supply of samples used in these investigations.